INÍCIO

DURATION OF WEATHERING EPISODES IN SMALL WATERSHEDS: IMPLICATION ON PLAGIOCLASE WEATHERING RATES

Pacheco FAL[1], Medina, J[2], Ribeiro, S[2], Van der Weijden CH[3]

[1]Department of Geology and Centre for Chemistry, Trás-os-Montes and Alto Douro University, Ap. 1013, 5000 Vila Real, Portugal, fpacheco@utad.pt.

[2]University of Aveiro 3810-193 Aveiro, Portugal, jmedina@ua.pt, sararibeiro@ua.pt

[3]Department of Earth Sciences—Geochemistry, Faculty of Geosciences, Utrecht University, P.O. Box 80.021 3508 TA Utrecht, The Netherlands, chvdw@geo.uu.nl.

Abstract

Spring watersheds were characterized for their morphological and hydrographical parameters using GIS, and depths of spring water circulation were determined using correlations between depths of conductive fractures measured in drilled wells and concomitant $^{87}Sr/^{86}Sr$ ratios in drilled well waters. Subsequently, mathematical approaches were used to estimate aquifer's hydraulic conductivities and effective porosities, and groundwater travel times, from measured spring discharge rates. Finally, a mole balance model was used to derive the relevant weathering reactions contributing to spring water composition. Combining all this data, plagioclase weathering rates could be calculated for each spring site and checked against literature results. Notwithstanding natural weathering is operating over geological time scales, the calculated rates follow the trend of experimental results that work on fresh materials, suggesting that current weathering episodes operating within the watersheds are not far from their starts. Different results are obtained when the analysis is focused on soil profiles.

Key-words: spring watershed, soil profile, plagioclase weathering rate, groundwater travel time.

Resumo

Bacias hidrográficas de nascentes foram caracterizadas relativamente aos seus parâmetros morfológicos e hidrográficos usando SIG, e as profundidades de circulação das águas de nascente foram determinadas utilizando correlações entre profundidades de fracturas condutoras medidas em furos e as razões $^{87}Sr/^{86}Sr$ das suas águas. Subsequentemente, aproximações matemáticas foram usadas para estimar condutividades hidráulicas e porosidades efectivas do aquífero fracturado, assim como tempos de circulação da água subterrânea, a partir dos registos de descarga das nascentes. Finalmente, um modelo de balanço de massa foi usado para derivar as reacções de alteração relevantes que determinaram a composição química das nascentes. Combinando todos estes dados foi possível calcular taxas de alteração da plagioclase para cada nascente e comparar os resultados com a literatura publicada. Não obstante a alteração natural ao nível das bacias hidrográficas operar continuamente ao longo dos tempos geológicos, as taxas calculadas seguem a tendência observada em trabalhos experimentais que lidam com materiais frescos, sugerindo que os episódios de alteração correntes não estão longe do seu início. Resultados diferentes obtêm-se quando a análise incide sobre perfis de alteração de solos.

Palavras-chave: bacia hidrográfica de nascente, perfil de alteração, taxa de alteração da plagioclase, tempo de percurso da água subterrânea.

1. Introduction

Weathering is a multi-scale and multi-stage process, whereby a fresh rock is converted into disaggregated plasma, and rates of mineral weathering determined by various methods reflect the differences in the temporal and geometric scales on which the approaches are standing. This paper is a contribution for the understanding of the weathering process of plagioclase at the spring watershed scale.

2. Study Area

The region of Vila Pouca de Aguiar is located in the North of Portugal and occupies an area of approximately 437 km^2. The geology of the area is characterized by Hercynian (syn- to post-tectonic) granites that intruded Palaeozoic (Cambrian to Devonian) metassediments and were covered by Quaternary alluvial and terrace deposits along a large-scale tectonic structure known as the Vila Real fault. The Vila Pouca de Aguiar granites are composed of quartz (31.5%), plagioclase (35.3), K-feldspar (26.7), biotite (4.4) and muscovite (1.4), with minor amounts of apatite and ilmenite. The plagioclase composition ranges from albite-An_8 to andesine-An_{37} (Pacheco et al., 1999). The metassediments, which include greywackes, phyllites, quartzites and graphitic slates, contain quartz, muscovite and smaller amounts of biotite, K-feldspar and albite-oligoclase (Pacheco, 1995). Climate in the area is temperate with wet-cold and dry-warm alternating seasons. The annual precipitations range from 900 mm/y in the Northeast to 1900 mm/y in the Southwest of the region (Figure 1).

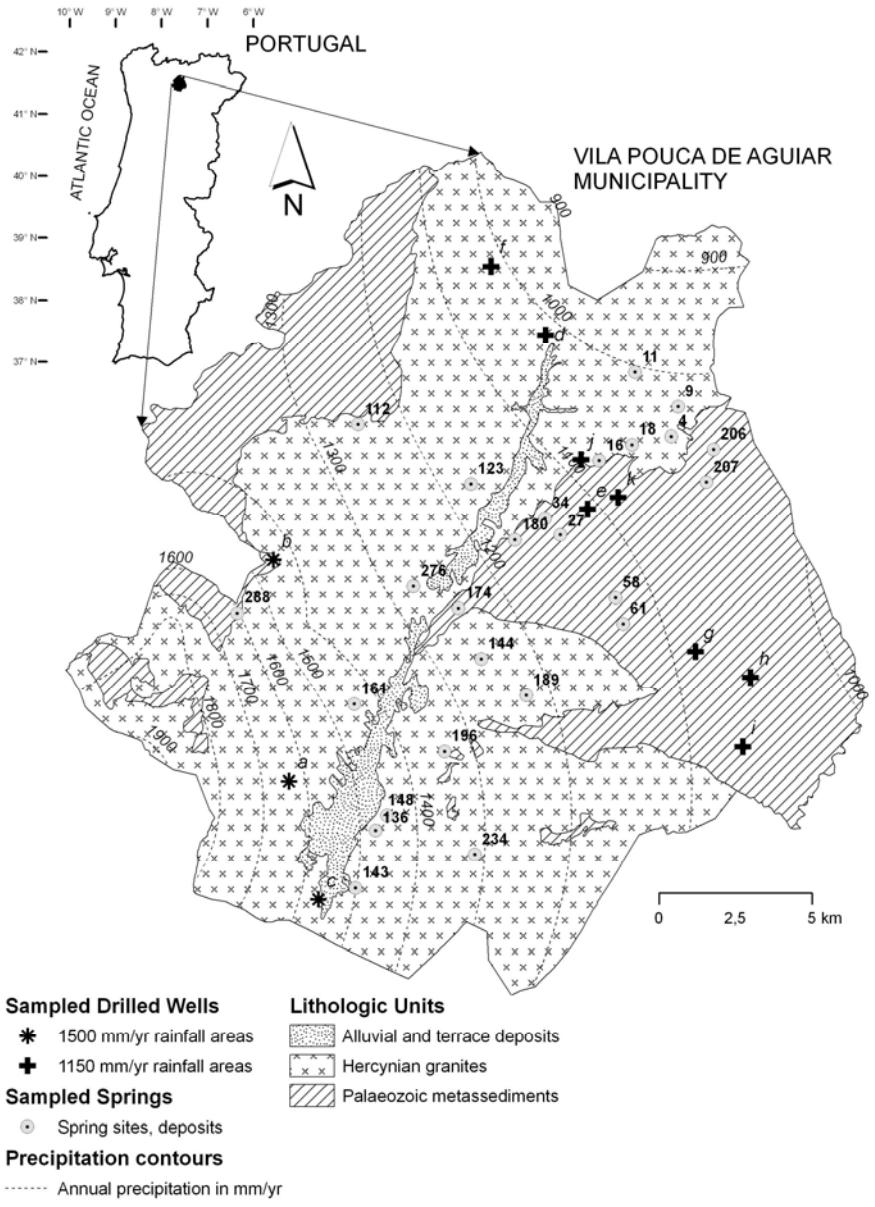

Figure 1 – Location and simplified geologic map of the Vila Pouca de Aguiar region. Distribution of the annual precipitation (contours), and of sampled drilled wells and springs. The labels close to the sampling sites are in agreement with the Nr codes in Tables 1a and 1b.

3. Borehole and Spring Water Chemistry

Samples of granite and metassediment springs were collected within the limits of the Vila Pouca de Aguiar municipality, in July–November 2007 for chemical analysis of major dissolved compounds and strontium, and in November 2007–June 2008 for isotopic analysis of strontium ($^{87}Sr/^{86}Sr$). Drilled well and rainwater samples were collected in October–December 2008 and January 2009, respectively, for analysis of $^{87}Sr/^{86}Sr$. The sampling sites are shown in Figure 1. At the sampling site, a water sample was collected and filtered through a 0.4 μm membrane filter. The filtered water was split into 4 portions: portions 1 and 2 were stored for chemical analysis at the laboratories of the Earth Sciences—Geochemistry department of the Utrecht University (The Netherlands), the first acidified with HNO_3 until pH ≤ 2; portion 3 was stored for isotopic analysis of strontium at the laboratory of isotope geology of the Aveiro University (Portugal), also acidified with HNO_3 until pH ≤ 2; and portion 4 was stored for analysis of alkalinity in the field laboratory, within 24 hours using the Gran plot method. Sodium, potassium, magnesium, calcium, and silicon were analyzed by ICP-OES in portion 1, while chloride, sulfate, and nitrate were determined by ion chromatography in portion 2. Approximately 50 ml of portion 3 were evaporated and the final residues were dissolved with 1ml HF and 0.5ml HNO_3 (both concentrated and sub-boilling distillated acids). After evaporation, these solutions were dissolved with HCl (6N) and dry. The strontium was separated from other elements of the matrix using conventional ion chromatography technique in ion exchange column with AG8 50W Bio-Rad cation exchange resin. All the intervenient reagents in the preparation of the samples were sub-boilling distillated, and the water produced by a Milli-Q Element (Millipore) apparatus. The strontium isotopic composition ($^{87}Sr/^{86}Sr$) was acquired in a Multi-Collector Thermal Ionisation Mass Spectrometer (TIMS) VG Sector 54. Sr was loaded on a single tantalum filament with H_3PO_4, and data were acquired at dynamic mode with peak measurements at 1-2V to ^{88}Sr. The isotopic ratios were corrected for mass fractionation relative to $^{88}Sr/^{86}Sr=0.1194$ and, during this study, the SRM-987 standard gave an average value of $^{87}Sr/^{86}Sr= 0.710249\pm6$; N=18; conf. lim.=95%. The analytical results for the springs and drilled wells are shown in Tables 1a and 1b. For rain water, $^{87}Sr/^{86}Sr = 0.7100076$.

4. Morphologic and Hydrographic Characterization of Stream and Spring Watersheds

The continuous shaping of the Earth's surface by meteoric water results in the development of watersheds that can be conceived at various scales depending on the order of the associated talweg (river, stream and streamlet). According to the classification of Strahler (1957), talwegs with no tributaries are termed 1st-order talwegs and are fed by 1st-order watersheds; the confluence of two i^{th}-order talwegs generates a $(i+1)^{th}$-order. The relationships between order and the morphologic and hydrographical features of the watersheds are firm and have been early recognized by Horton (1945).

For the region of Vila Pouca de Aguiar, watersheds of order 1 to 3 were drawn using a GIS software (ArcHydro; ESRI, 2007), and the relationships between order and the watershed's area (A, m^2), volume (V, m^3) and length of talwegs (L, m) were determined (Figure 2).

Springs emerge in the vicinity of talwegs, but not necessarily in the talwegs. Usually, the neighbour talwegs are not all of the same order and therefore the watersheds of springs are classified according to the concept of equivalent order (i_{eq}), which is the ratio of the length of talwegs surrounding the spring to a predefined extent (L, m), weighted according to their order, to the length of those talwegs unweighted:

$$i_{eq} = \frac{\sum_{i=1}^{n} L_i \times i}{L} \quad (1)$$

Table 1a – Annual discharge (V_r), integrated from measured discharge rates on a monthly basis, and chemical and isotopic composition of the sampled springs.

NR	V_r	$[Na^+]$	$[K^+]$	$[Mg^{2+}]$	$[Ca^{2+}]$	$[HCO_3^-]$	$[Cl^-]$	$[SO_4^{2-}]$	$[NO_3^-]$	$[H_4SiO_4^0]$	$^{87}Sr/^{86}Sr$
	m^3/y	μmol/L									
4	15404	259	12	25	35	216	128	11	0	420	0.7297446
9	14295	296	23	48	121	408	154	29	0	387	0.7288604
11	19955	248	16	34	60	241	132	16	0	353	0.7237384
16	8056	337	29	57	51	394	129	10	0	452	0.7259299
18	26207	181	16	40	18	156	117	6	0	240	0.7297766
27	11615	136	23	76	30	111	158	17	14	141	0.7282520
34	6958	116	13	52	24	124	116	22	2	146	0.7296706
58	6822	98	35	34	17	40	125	4	50	112	0.7308898
61	7204	132	6	53	21	86	145	6	17	132	0.7224757
112	3608	121	8	9	9	35	109	2	12	137	0.7291700
123	32250	387	14	46	176	462	179	21	0	421	0.7152858
136	6686	202	7	12	28	141	140	4	0	258	0.7274434
143	26457	138	4	8	15	89	104	1	10	187	0.7290213
144	16175	101	3	6	9	5	114	2	6	87	0.7273776
148	48044	131	3	8	14	53	109	3	8	152	0.7296969
161	27443	183	6	17	50	191	114	10	0	227	0.7179070
174	23738	203	25	77	35	243	117	41	0	304	0.7288553
180	25438	148	21	63	37	164	118	35	0	253	0.7286865
189	81932	142	0	11	14	16	132	3	12	148	0.7314792
196	27667	214	5	16	24	98	131	5	6	248	0.7310440
206	10093	126	16	50	43	181	134	3	54	133	0.7289179
207	6892	110	12	42	24	50	117	3	68	89	0.7277835
234	32421	114	3	7	14	48	96	2	0	163	0.7241002
276	31269	117	2	12	25	54	82	15	10	118	0.7262283
288	5950	172	12	39	32	191	123	1	5	235	0.7208825

Table 1b – Depth of conductive fractures (D_{med}) measured in drilled wells. Rainfall (P) around the sampling sites. $^{87}Sr/^{86}Sr$ ratios of the drilled well waters.

NR	D_{med}	P	$^{87}Sr/^{86}Sr$
	m	mm/y	
a	32	1500	0.722366
b	42		0.726328
c	78		0.737331
d	27	1150	0.716282

e	39		0.715500
f	44		0.716820
g	75		0.721164
h	81		0.718847
i	87		0.724840
j	88		0.720075
k	96		0.729103

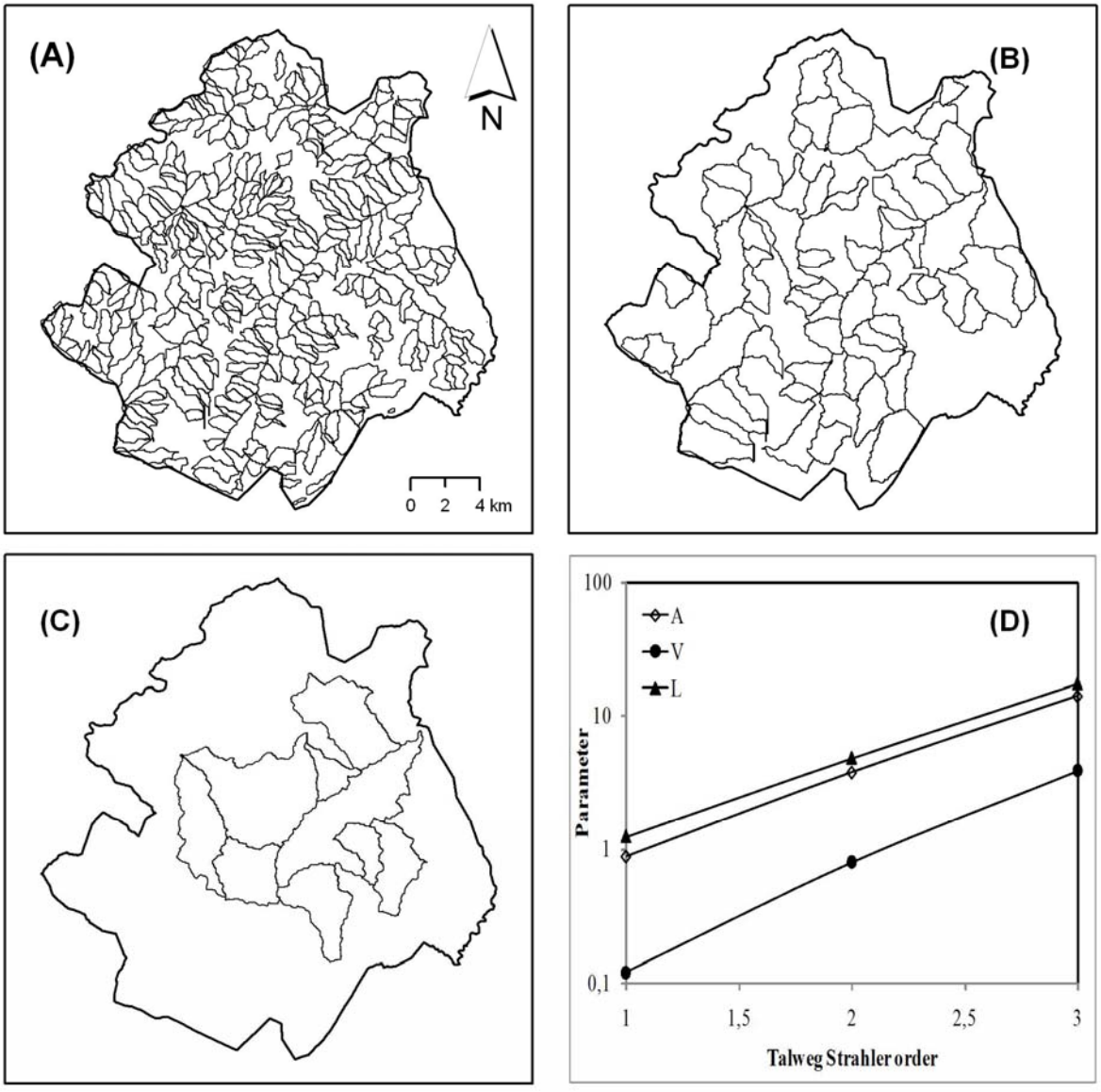

Figure 2 – Distribution of watersheds within the Vila Pouca de Aguiar region: (A) order-1 talwegs, (B) order-2 talwegs, and (C) order-3 talwegs. Relationships between order (i) and the morphological and hydrographical parameters of the watershed: (D) watershed area – A (km^2) = $0.2233e^{1.3911i}$; watershed volume – V (km^3) = $0.0221e^{1.7406i}$; length of talwegs within the watershed – L (km) = $0.3339e^{1.3217i}$. Orders of the talwegs established according to the classification of Strahler (1957). All relationships are associated to a coefficient of determination $R^2 = 0.99$.

Unlike talweg orders, which are integers, equivalent talweg orders are real values. When a spring site falls in a region where, for example, $i_{eq} = 1.5$, this means that the catchment area of

the spring is larger than the average area of 1st-order watersheds and smaller than the average area of 2nd-order watersheds.

Equivalent talweg orders were calculated for the entire region of Vila Pouca de Aguiar using Equation 1 (Figure 3), from which the concomitant orders of the sampled springs were deduced. These orders were subsequently applied to the relationships defined in Figure 2, allowing for the calculation of the spring's catchment area, volume and length of talwegs (Table 2).

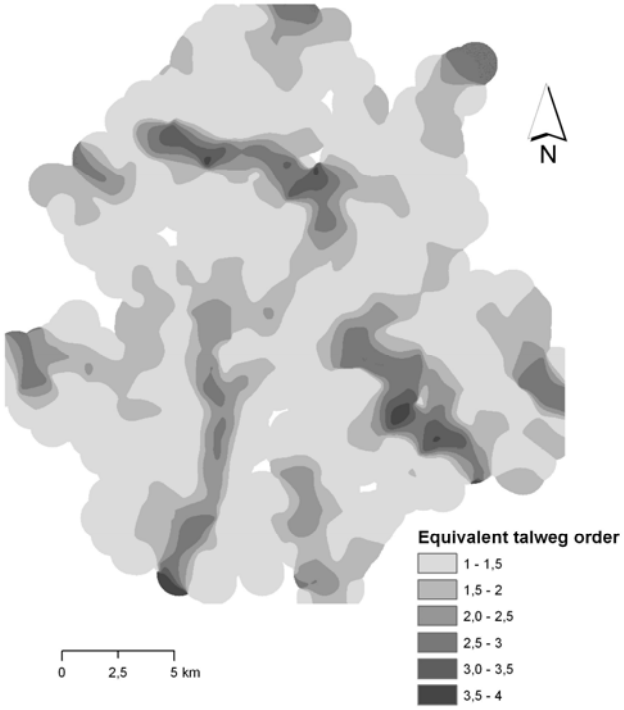

Figure 3 – Distribution of equivalent talweg orders within the Vila Pouca de Aguiar region.

5. Depths of Hydraulic Circuits

Precipitation water infiltrates the subsoil to a certain depth determined by the aquifer formation constants (hydraulic conductivity and effective porosity) and the saturation state of the system. Usually, the maximum depth corresponds to the average topographic thickness of the watershed ($D = V/A$), but the actual depth is just a fraction of this value (δ) unless fracturing is very intense and pervasive.

The average depths of conductive fractures of the sampled drilled wells are listed in Table 1b (D_{med}), ranging from a minimum of 27 to a maximum of 96 meters. These depths are viewed as depths of groundwater pathways across the local granite and metassediment aquifers. Depending on whether the boreholes were located in areas of lower (P_{min} = 1150 mm/y) or higher (P_{max} = 1500 mm/y) rainfall, different correlations were established between the D_{med} values and the concomitant $^{87}Sr/^{86}Sr$ ratios in the drilled well waters (Figure 4). Subsequently, these correlations were used to estimate the depth of circulation of the spring waters (D_z), in keeping with their $^{87}Sr/^{86}Sr$ ratios (Table 1), as follows:

$$D_z = \frac{(P - P_{min})(D_{max} - D_{min})}{P_{max} - P_{min}} + D_{min} \quad (2)$$

where P is the annual precipitation around the spring site (Table 1) and D_{max} and D_{min} are deduced from the regression equations shown in Figure 4, i.e.:

$$D_{min} = \frac{^{87}Sr/^{86}Sr(spring) - ^{87}Sr/^{86}Sr\,(rain)}{1.527 \times 10^{-4}} \quad (3a)$$

$$D_{max} = \frac{^{87}Sr/^{86}Sr(spring) - ^{87}Sr/^{86}Sr\,(rain)}{3.621 \times 10^{-4}} \quad (3b)$$

Table 2 – Results of the hydrological and weathering modelling approaches. Symbols: NR – identification code of the spring site; A, V and L – associated watershed area, topographic volume and length of talwegs; D_z, V_z and δ – average depth of spring water circulation, volume of water interacting with percolating spring water and ratio between V_z and V; K and n_e – hydraulic conductivity and effective porosity of the fractured media; t – groundwater travel time (equated to the mean turnover time); [Pl] and W_{Pl} – moles of plagioclase dissolved in the process of weathering and concomitant weathering rates.

NR	A x10^5	V x10^8	L	D_z	δ	V_z x10^8	K x10^{-8}	n_e x10^{-2}	t	[Pl]	W_{Pl} x10^{-15}
	m^2	m^3	m	m		m^3	m/s		y	µmol/L	mol/m^2.s
4	8.975	1.259	1252	141.4	1.0	1.269	0.66	0.21	17.0	139	0.91
9	8.975	1.259	1252	138.4	1.0	1.242	0.73	0.11	9.5	nd	nd
11	17.950	2.518	2504	101.3	0.7	1.818	1.55	0.03	3.1	146	19.55
16	8.975	1.259	1252	97.7	0.7	0.877	1.16	0.17	18.1	242	2.20
18	35.166	5.335	4833	129.6	0.9	4.558	0.49	0.01	1.8	82	20.16
27	10.282	1.492	1425	101.6	0.7	1.044	1.94	0.02	1.6	28	11.46
34	18.942	3.205	2546	108.2	0.6	2.050	0.55	0.01	3.2	53	7.28
58	14.677	2.329	1998	123.6	0.8	1.815	0.64	0.02	4.0	38	3.91
61	21.779	3.816	2907	72.8	0.4	1.586	1.29	0.02	3.9	52	7.16
112	9.207	1.300	1283	78.1	0.6	0.719	0.36	0.02	4.9	nd	nd
123	17.950	2.518	2504	26.3	0.2	0.472	30.76	0.69	10.1	nd	nd
136	33.401	5.649	4496	70.2	0.4	2.344	0.75	0.03	9.1	88	3.26
143	29.996	4.787	4079	77.0	0.5	2.311	4.06	0.09	8.1	58	2.96
144	8.975	1.259	1252	89.1	0.6	0.800	5.54	0.06	2.8	nd	nd
148	8.975	1.259	1252	89.2	0.6	0.801	28.18	0.27	4.4	nd	nd
161	48.205	8.012	6509	28.9	0.2	1.391	8.76	0.08	4.2	127	19.22
174	19.763	2.844	2744	94.9	0.7	1.875	2.19	0.06	5.1	111	7.97
180	17.950	2.518	2504	99.0	0.7	1.777	1.37	0.07	4.8	70	4.07

189	8.975	1.259	1252	119.1	0.8	1.069	12.83	0.18	2.3	nd	nd
196	8.975	1.259	1252	100.6	0.7	0.903	3.28	0.17	5.5	83	4.09
206	26.925	3.777	3757	141.8	1.0	3.818	0.16	0.04	15.2	57	0.46
207	9.948	1.432	1381	127.2	0.9	1.266	0.76	0.06	11.2	24	0.47
234	66.479	10.905	8992	71.0	0.4	4.719	1.66	0.10	13.9	nd	nd
276	85.590	14.645	11500	62.6	0.4	5.358	0.51	0.39	66.7	43	0.05
288	8.975	1.259	1252	20.0	0.1	0.179	6.68	31.13	9.4	117	3.60

The calculated values of D_z (Table 2) range from a minimum of 20 to a maximum of 142 m, being on average 92±34 m. Comparative to the average topographic thicknesses (V/A = 150±12 m) they represent solely a fraction δ = 63±25 %. In further calculations using the volume of groundwater involved in weathering reactions (V_z), this volume will be defined in keeping with these results, i.e.:

$$V_z = \delta V \tag{4}$$

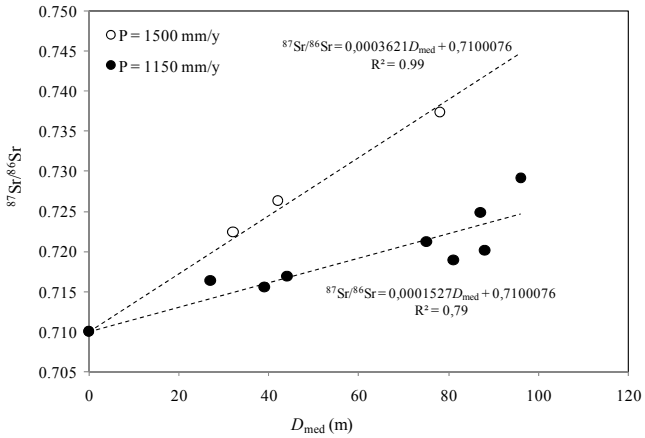

Figure 4 – Correlations between the $^{87}Sr/^{86}Sr$ ratios and D_{med}.

6. Aquifer Formation Constants and Groundwater Travel Times

The estimation of hydraulic conductivities (K, m/y) and effective porosities (n_e, dimensionless) employed the Brutsaert method (Brutsaert and Lopez, 1998). According to this method, in a graphical plot of discharge rate (Q, m^3/s) and time (t, s) measurements – $\ln(\Delta Q/\Delta t)$ *vs*. $\ln(Q)$ – the lower envelope to the scatter points is represented by two straight lines, one of slope b =1 and the other of slope b = 3, with intercept-y values (a_1, a_3) related to K and n_e as follows:

$$K = 0.57\sqrt{\frac{a_3}{a_1}}\left(\frac{A^3}{V_z^{\,2}L^2}\right) \tag{5a}$$

$$n_e = \frac{1.98}{V_z\sqrt{a_1 a_3}} \tag{5b}$$

The method is illustrated in Figure 5 for spring site nr 144. For this station, $K = 5.54\times10^{-8}$ m/s and $n_e = 6.0\times10^{-2}$, on average $K = (4.7\pm7.9)\times10^{-8}$ m/s and $n_e = (1.4\pm6.1)\times10^{-2}$ (Table 2). These values are representative of fractured rock hydraulic conductivities and effective porosities. The discharge rate measurements on which the calculations of K and n_e are standing are presented elsewhere.

The concept of hydraulic turnover time (McGuire and McDonnell, 2006) was used to estimate the mean travel time (t, s) of groundwater within the watershed boundaries. This time is the ratio of the mobile watershed storage ($V_z n_e$, m^3) to the volumetric flow rate (V_r, m^3 in one year):

$$t = \frac{V_z n_e}{V_r} \tag{6}$$

For station 144, $t = 2.8$ y, on average 9.6±12.6 y (Table 2).

7. Weathering Model

It was assumed that, in the process of chemical weathering, plagioclase and biotite are the major contributors to the chemistry of springs. The conceptual mole-balance model (SiB algorithm of Pacheco and Van der Weijden, 1996, Pacheco et al., 1999) set the weathering of plagioclase into mixtures of kaolinite and gibbsite because rainfall in the area is always higher than 1000 mm/y (Martins et al., 1995; Van der Weijden and Pacheco, 2006), and set the weathering of biotite into mixtures of kaolinite and vermiculite. The results relative to plagioclase mole fractions ([Pl], mol/L) are depicted in Table 2.

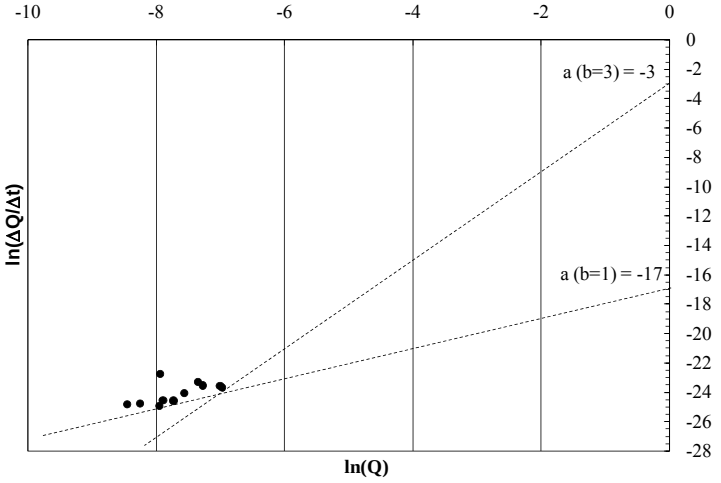

Figure 5 – Application of the Brutsaert method to spring site nr 144.

8. Plagioclase Weathering Rates and the Duration of Weathering Episodes

Plagioclase weathering rates can be determined with the formula (Pacheco and Van der Weijden, 2009):

$$W_{Pl} = \frac{[\mathrm{Pl}]}{2 \times t \times \alpha_{Pl}} \sqrt{\frac{12 \mu_w K}{\rho_w g n_e}} \tag{7}$$

where α_{Pl} is the proportion of plagioclase in the rocks, ρ_w(kg/m^3) and μ_w(kg/s·m) are the specific weight and dynamic viscosity of water (at T = 15ºC, ρ_w = 999.1 kg/m^3, and μ_w = 1.14 × 10^{-3} kg/s·m), g (9.81 m/s^2) is the acceleration of gravity. Considering that most spring waters circulate in granite environment, it was assumed that α_{Pl} = 0.35. Rates calculated by Equation 7 for all the springs are listed in Table 2 (last column), being on average (5.7±5.6) × 10^{-15} mol/m^2·s.

White and Brantley (2003) investigated the effect of time on the weathering of plagioclase and concluded that concomitant rates decrease according to a power function of the duration of weathering. This function is identified in Figure 6 as "average trend". However, laboratory experiments reveal that at initial stages of weathering plagioclase dissolution rates fit to a steeper power function indentified as "initial trend".

The duration of weathering is unknown within the springs' watersheds. However, it is certain that each spring water sample is one after many other fluid packets that already flew across the local granite and metassediment aquifers. It is striking then how plagioclase weathering rates calculated for the springs (filled circles) fit to the initial trend. Apparently, notwithstanding weathering is continuously happening within the watershed, meaning that the duration of weathering is larger than the groundwater travel time used to produce the plot of the springs, every new fluid packet seems to invade unweathered sectors of the massif and therefore to represent a "initial" stage of weathering.

In most studies, the duration of weathering episodes comprises the time required by water to convert a fresh rock into a soil or saprolite, and is most commonly determined from distributions of cosmogenic isotopes leading to ages up to 3.02×10^{-6} y (White and Brantley, 2003). However, the process of soil and saprolite formation involves solely a small portion of the watershed volume. An attempt to extend the isotopic approach to the scale of a watershed would undoubtedly result in much longer times. The differences in scale resulting from studies focused at the soil profile or at the watershed might after all explain why the filled circles follow the steeper trend line. Eventually, this is because weathering in the spring watersheds although is occurring over geological time scales, the episodes are just starting given the awesome volumes of rock that have to be broken apart.

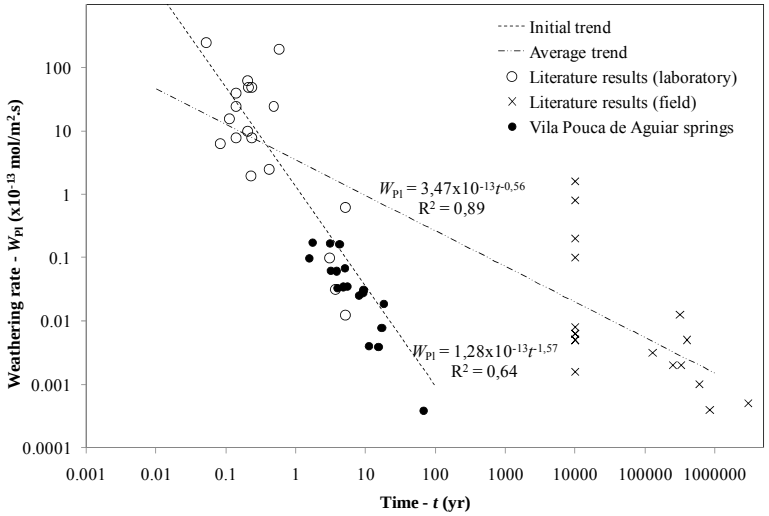

Figure 6 – Plagioclase weathering rates and the duration of weathering episodes. For the literature results and trends, time is the duration of weathering, for the Vila Pouca de Aguiar springs time is the travel time.

References

Brutsaert, W., Lopez, J.P. (1998). Basin-scale geohydrologic drought flow features of riparian aquifers of the southern Great Plains. *Water Resour. Res.* 30: 2759–2763.

ESRI (2007). *ArcHydro tools - tutorial*, version 1.2, for ArcInfo 9.2. ESRI, Redlands, USA, 110pp.

Horton, R. E. 1945. Erosional development of streams and their drainage basins: hydrophysical approach to quantitative morphology. *Geological Society of America Bulletin* 56:275-370.

McGuire, K.J., McDonnell, J.J. (2006). A review and evaluation of catchment transit time modelling. *J. Hydrol.* 330: 543-563.

Martins, A.A.A., Madeira, M.V., Refega, A.A.G. (1995). Influence of rainfall on properties of soils developed on granite in Portugal. Arid Soil Research and Rehabilitation, 9: 353–366.

Pacheco, F.A.L. (1995) *Interacção Água-Rocha em Unidades do Grupo Peritransmontano (Serra da Padrela-Vila Pouca de Aguiar).* Tese de Mestrado, Universidade de Coimbra, Coimbra, 123p.

Pacheco, F.A.L., Van der Weijden, C.H. (1996). Contributions of water-rock interactions to the composition of ground water in areas with sizeable anthropogenic input. A case study of the waters of the Fundão area, central Portugal. *Water Resour. Res.* 32: 3553–3570.

Pacheco, F.A.L., & Van der Weijden, C.H., (2009, submetido). *Hydrologic and kinetic modeling of plagioclase weathering rates in the Vouga basin (Portugal): reconciling field and laboratory rates.* Geophysics, Geochemistry and Geosystems (G^3).

Pacheco, F.A.L., Sousa Oliveira, A., Van der Weijden, A.J., Van der Weijden, C.H. (1999). Weathering, biomass production and ground water chemistry in an area of dominant anthropogenic influence, the Chaves-Vila Pouca de Aguiar region, north of Portugal. *Water Air Soil Poll.* 115: 481–512.

Strahler, A. N. (1957). Quantitative Analysis of Watershed Geomorphology. *Transactions of the American Geophysical Union* 8 (6): 913–920.

Van der Weijden, C.H., Pacheco, F.A.L. (2006). Hydrogeochemistry in the Vouga River basin (central Portugal): pollution and chemical weathering. *Appl. Geochem.* 21: 580–613.

White, A.F., Brantley, S.L. (2003). The effect of time on the weathering of silicate minerals: why do weathering rates differ in the laboratory and field? *Chem. Geol*. 202: 479–506.